J. Membrane Biol. 213, 111–118 (2006)
DOI: 10.1007/s00232-006-0879-3

The Journal of
Membrane
Biology



# Mechanism and Putative Structure of $B^0$-like Neutral Amino Acid Transporters

**M. O'Mara[1], A. Oakley[2], S. Bröer[3]**
[1]Dept. of Biological Sciences, University of Calgary, 2500 University Dr. NW, Calgary, Alberta, Canada, T2N 1N4
[2]Research School of Chemistry, Australian National University, Canberra, ACT 0200, Australia
[3]School of Biochemistry & Molecular Biology, Australian National University College of Science Canberra, ACT 0200, Australia

Received: 10 November 2006

**Abstract.** The $Na^+$-dependent transport of neutral amino acids in epithelial cells and neurons is mediated by $B^0$-type neutral amino acid transporters. Two $B^0$-type amino acid transporters have been identified in the neurotransmitter transporter family SLC6, namely $B^0AT1$ (SLC6A19) and $B^0AT2$ (SLC6A15). In contrast to other members of this family, $B^0$-like transporters are chloride-independent. $B^0AT1$ and $B^0AT2$ preferentially bind the substrate prior to the $Na^+$-ion. The $Na^+$-concentration affects the $K_m$ of the substrate and vice versa. A kinetic scheme is proposed that is consistent with the experimental data. An overlapping binding site of substrate and cosubstrate has been demonstrated in the bacterial orthologue $LeuT_{Aa}$ from *Aquifex aeolicus*, which elegantly explains the mutual effect of substrate and cosubstrate on each other's $K_m$-value. $LeuT_{Aa}$ is sequence-related to transporters of the SLC6 family, allowing homology modeling of $B^0$-like transporters along its structure.

**Key words:** Hartnup disorder — Neurotransmitter transporter — Structure modeling — SLC6A19 — SLC6A15

## Functional Properties of System $B^0$ in Kidney and Intestine

Epithelial cells use the $Na^+$-electrochemical gradient to accumulate metabolites in the cytosol and subsequently release metabolites across the basolateral membrane, using antiport and uniport mechanisms (Crane, 1965; Schultz & Curran, 1970). Kidney and intestine express similar sets of transporters reflecting the role of epithelial cells as sites of metabolite absorption (Binder, 1970).

Functional studies performed in the 60's and 70's demonstrated the presence of a dominant $Na^+$-dependent neutral amino acid transport activity in epithelial cells of kidney and intestine, as supported by the following observations. Removal of $Na^+$ abolishes the accumulation of neutral amino acids in kidney slices (Fox et al., 1964; Scriver & Mohyuddin 1968; Segal & Crawhall 1968), abolishes transepithelial transport of neutral amino acids in perfused tubules (Ullrich et al., 1974) and prevents the overshoot phenomenon in vesicles (Evers et al., 1976; Fass et al., 1977). In the intestine, transport of neutral amino acids is entirely $Na^+$-dependent and no accumulation is observed in the absence of $Na^+$ (Cohen & Huang, 1964; Reiser & Christiansen, 1967; Schultz et al., 1967). A $1Na^+$:1substrate cotransport stoichiometry was reported for phenylalanine and alanine (Fass et al., 1977; Kragh-Hansen et al., 1984; Hoyer & Gogelein 1991), which is consistent with the observation of inward currents during neutral amino acid transport in intact rat proximal tubule (Samarzija & Fromter, 1982). It appears that increased extracellular $Na^+$ mostly affects the $K_m$ of the substrate rather than the $V_{max}$ of the transport process (Curran et al., 1967; Evers et al., 1976; Fass et al., 1977). This transport activity for neutral amino acids was proposed to be mediated by a single transporter referred to as system $B^0$ (for broad neutral) or NBB (for neutral brush border) (Preston et al., 1974; Paterson et al., 1981; Doyle & McGivan, 1992). This notion was based on mutual competition between most neutral amino acids, as observed in experiments using intestinal and renal preparations and by the excretion of almost all neutral amino acids in Hartnup disorder (Cusworth & Dent, 1960; Potter et al., 2002), which was later shown to be caused by

*Correspondence to:* S. Bröer; email: stefan.broeer@anu.edu.au
*Abbreviations:* BCH, 2-aminobicyclo[2,2,1]heptane-2-carboxylic acid; NMDG, N-methyl-D-glucamine.

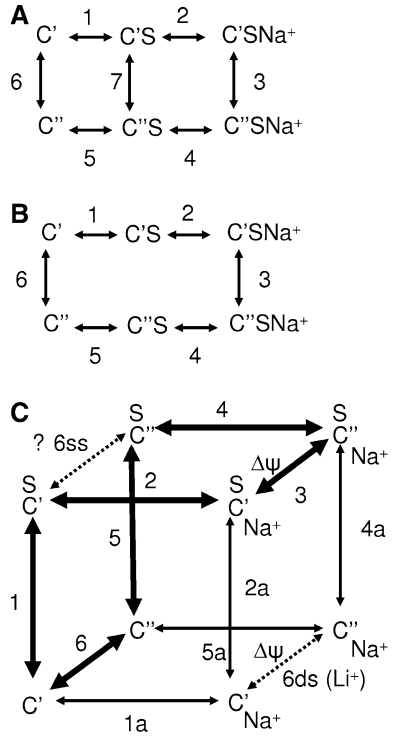


**Fig. 1.** Kinetic schemes for the intestinal amino acid transport system $B^0$ and its molecular correlate $B^0AT1$. Association and dissociation of substrate and cosubstrate are not depicted. Substrate is denoted by 'S'. The two orientations of the carrier (C) are denoted as (C') and (C''). Voltage-dependent steps are indicated by $\Delta\psi$. (*A*) Kinetic scheme for intestinal alanine transport as proposed by Curran et al. (Curran et al., 1967). (*B*) Kinetic scheme as proposed by Camargo et al. (Camargo et al., 2005). (*C*) Novel scheme for the transport mediated by $B^0AT1$; for details *see* text.

mutations in the system $B^0$ transporter (Kleta et al., 2004; Seow et al., 2004).

Functional studies, in particular those using intact intestinal mucosa, resulted in the first formulation of a kinetic mechanism for system $B^0$ (Curran et al., 1967). The model (Fig. 1*A*) comprises the following features: (i) Transport is independent of the intracellular $Na^+$ concentration. (ii) At constant $Na^+$, substrate transport follows Michaelis-Menten kinetics. (iii) Substrate $V_{max}$ is independent of the extracellular $Na^+$ concentration. (iv) Substrate transport can occur in the absence of $Na^+$ with low affinity. (v) The substrate $K_m$ decreases with increasing $Na^+$ concentration. (vi) The transporter does not show trans-stimulation. The model fits the experimental data on intestinal alanine transport and assumes equal permeabilities for the empty, substrate-loaded and fully loaded transporter (i.e., the rate constants of steps *3, 6* and *7* in Fig. 1*A* are equal) in the absence of a membrane potential.

Introduction of a membrane potential will change the permeability of the voltage-dependent step 3. This model further predicts that the substrate binds prior to the $Na^+$-ion (Schultz & Curran, 1970), because the carrier is thought to mediate substrate transport also in the absence of $Na^+$. In Fig. 1*A* the $Na^+$-independent transport would entail steps *1-7-5-6*, whereas $Na^+$-driven transport entails steps *1-2-3-4-5-6*. As pointed out above, $Na^+$-dependent and $Na^+$-independent transport cycles would be equally fast in the absence of a membrane potential. In the presence of an inside-negative membrane potential cycle *1-2-3-4-5-6* would be significantly faster than cycle *1-7-5-6*. The model is, however, inconsistent with the data in respect to the observation that substrate $V_{max}$ is independent of the extracellular $Na^+$ concentration. In a transport cycle $V_{max}$ is determined by the ligand that binds last to the transporter (i.e., $Na^+$ in this model) (Stein, 1986). If this ligand is present at saturating concentration, $V_{max}$ is reached, because all transporters are fully loaded and able to undergo the conformational change required for substrate translocation. Lower concentrations result in partial saturation and reduced velocity. If the first binding ligand (i.e., the substrate in Fig. 1*A*) is present at subsaturating concentrations, $V_{max}$ can still be reached by saturating concentrations of the second ligand ($Na^+$). If the diffusion of substrate and cosubstrate is much faster than the conformational change of the transporter, the supply of transporters loaded with ligand 1 is not rate limiting although only a fraction of carriers maybe loaded with this ligand (Stein 1986).

In earlier studies it has been suggested that cationic and anionic amino acids also interact with system $B^0$ albeit with lower affinity (Schultz et al., 1970; Schultz & Curran, 1970). In this model the positive charge of cationic amino acids could replace the requirement for $Na^+$-cotransport. As a result, transport of cationic amino acids would be $Na^+$-independent but of low affinity. Anionic amino acids on the other hand would be transported at low pH in a $Na^+$-dependent manner. The interaction of cationic and anionic amino acids with the transporter was later shown to be very weak (Preston et al., 1974), excluding a physiological role of system $B^0$ in the transport of charged amino acids. It is now well established that anionic and cationic amino acids are taken up into epithelial cells by separate transporters (Palacin et al., 2005). A weak interaction of charged amino acids with system $B^0$ could also be caused by competition of several transporters for the sodium electrochemical gradient. For example, high concentrations of D-glucose also inhibit amino acid uptake (Mircheff et al., 1982; Murer et al., 1975) because glucose uptake is mediated by a $Na^+$-dependent transporter. Experiments in cultured cells, in particular, suggest that neutral amino acids are the only substrates of system $B^0$ (Doyle & McGivan, 1992). A correlation was established showing a decreased substrate $K_m$ with larger side chains (Preston et al., 1974). The correlation is particularly striking for amino acids with a linear side chain from glycine to norleucine. As a result, phenylalanine, methionine and leucine have low $K_m$

values for the neutral amino acid transporter (ranging from 1.5–4 mM), whereas alanine (16 mM) and particularly glycine have higher $K_m$ values.

The $B^0$-like transport mechanism was further characterized by Hoyer and Gogelein (Hoyer & Gogelein, 1991). They confirmed that increased $Na^+$ concentrations affect the $K_m$ for the substrate but not its $V_{max}$. They furthermore showed that the $Na^+$-$K_m$ decreased with hyperpolarization of the membrane. This was interpreted in terms of an ion-well effect. The maximum velocity is strongly potential-dependent, suggesting that the translocation step itself is voltage dependent.

## Properties of the Cloned System $B^0$ Neutral Amino Acid Transporter $B^0AT1$ (SLC6A19)

Two cDNAs encode transporters with properties similar to system $B^0$, namely $B^0AT1$ and $B^0AT2$. The molecular correlate of the intestinal and kidney system $B^0$ is $B^0AT1$ (SLC6A19) (Broer et al., 2004), a protein of 634 amino acids. The human SLC6A19 (Kleta et al., 2004; Seow et al., 2004) shows very little activity in heterologous expression systems. As a result, the mouse transporter has been characterized in more detail.

### Stoichiometry

In agreement with the functional data from kidney and intestine, a stoichiometry of $1Na^+$:1amino acid was suggested by the following evidence (Bohmer et al., 2005; Camargo et al., 2005). (i) Activation of leucine transport by increase in $Na^+$ concentrations shows a hyperbolic dependence, and (ii) uptake of leucine under voltage-clamp conditions shows translocation of 1 charge/leucine. The initially reported sigmoidal dependence of leucine transport on the $Na^+$ concentration (Broer et al., 2004) is a result of an inhibition of $Na^+$-binding by NMDG (Bohmer et al., 2005). The transporter is $Na^+$-dependent; replacing NaCl by NMDG-Cl completely abolishes transport. Replacement of NaCl by LiCl also abolishes uptake of radiolabelled substrate, however, substrate-induced currents are still observed, reaching 40% of the currents in the presence of $Na^+$. It appears that $Li^+$ causes a partial uncoupling of substrate and ion transport. Moreover, a substrate-independent $Na^+$ conductance is observed in $mB^0AT1$-expressing oocytes (Camargo et al., 2005).

### Interaction Between Substrate and Cosubstrate

As pointed out above it has consistently been reported that substrate transport via system $B^0$ displays a substrate $K_m$ that is dependent on the $Na^+$ concentration, whereas $V_{max}$ appears to be unaltered. The cloned mouse transporter shows the decrease of the substrate $K_m$ with increasing $Na^+$ concentration, but it also shows a reduction of $V_{max}$ at low $Na^+$ (Bohmer et al., 2005; Camargo et al., 2005). Vice versa, the cloned transporter also displays a decreased $K_m$ for $Na^+$ at increased substrate concentration. Thus, substrate and cosubstrate influence each other's binding, pointing to an overlapping binding site. There is disagreement between the studies whether a reduced substrate concentration also affects the $V_{max}$. Camargo et al. suggest that $V_{max}$ is reached at high $Na^+$ concentration, regardless of the prevalent substrate concentration (Camargo et al., 2005). Boehmer et al., by contrast, report a reduction of the maximum velocity at low substrate concentration (Bohmer et al., 2005). As a result, Camargo et al. propose an ordered binding mechanism in which substrate binds first (Fig. 1*B*), whereas Boehmer et al. propose a random binding order with a preference for substrate binding first. The influence of substrate and cosubstrate concentration on the maximum velocity remains a matter of debate and is not consistent between earlier functional studies and the properties of the cloned transporter.

### Voltage Dependence of $K_m$ and $V_{max}$

In agreement with an ion-well effect, a reduction of the $Na^+$-$K_m$ was reported at hyperpolarized membrane potential (Bohmer et al., 2005; Camargo et al., 2005). A reduction of the substrate $K_m$ was observed at hyperpolarized membrane potential, as well. This could relate to the ion-well effect exerted on $Na^+$-ions by the membrane potential. The increase of the local $Na^+$ concentration would in turn increase the affinity for the substrate. This scenario would require $Na^+$ to bind first to the transporter, which is at variance with the preferred order of binding. Alternatively, the membrane potential could also affect the conformation of the empty carrier, inducing a 'high affinity' state. The experimental data rather suggest that the membrane potential acts on the fully loaded transporter (Bohmer et al., 2005), a notion that is also supported by the lack of trans-stimulation (*see* below). The effect of the membrane potential could be explained if substrate and $Na^+$ would diffuse to the binding site as an ion pair, which still would carry a net positive charge.

### Substrate Specificity

$B^0AT1$ transports all neutral amino acids, albeit to a different extent. $V_{max}$-values vary only by a factor of 2, but affinities are different for each amino acid (Bohmer et al., 2005; Camargo et al., 2005). The order of preference is Met = Leu = Ile = Val > Gln = Asn = Phe = Cys = Ala > Ser = Gly = Tyr = Thr = His = Pro > Trp > Lys. This

order is in partial agreement with studies in the intestine (Paterson et al., 1979; Preston et al., 1974) and the kidney cell line NBL-1 (Doyle & McGivan 1992). The transporter shows some affinity for lysine; whether the transporter also interacts with anionic amino acids at low pH (Schultz & Curran 1970) remains to be shown. $B^0AT1$ is partially inhibited by BCH, an amino acid analogue with a bulky side-chain.

### A Kinetic Model for $B^0AT1$

All properties reported for $B^0$-like transport can be incorporated into a model with random binding order (Fig. 1*C*), which is similar to the general cotransporter model discussed by Stein (Stein, 1986). The coupled reaction of the transporter involves steps *1-2-3-4-5-6* (in the preferred order substrate first) or in the less preferred order ($Na^+$ first) involving steps *1a-2a-3-4a-5a-6*. Please note that no experimental data are available concerning the binding order at the cytosolic face of the transporter. For simplicity, symmetry is assumed, but the model allows any combination. The substrate-independent $Na^+$ conductance would comprise steps *1a-6ds-5a-6*. The substrate-induced lithium current would first require binding of the substrate, which is the preferred route. In contrast to the $Na^+$-driven cycle, step *3* cannot be concluded in the presence of lithium. Instead, binding of lithium would force the substrate to dissociate (step *2a*) and would subsequently follow the same route as the $Na^+$-leak current (steps *1-2-2a-6ds-5a-6*). Using a convention recently proposed by Nathan Nelson (Nelson et al., 2002) we call this cycle the drive-slip (ds) to indicate that the driving cation slips through without being accompanied by the substrate. The critical step is therefore denoted *6d*s. In addition, a substrate slip can be proposed involving steps *1-6ss-5-6*. The critical step in this cycle would be *6ss* (substrate slip). Although a substrate slip has not been observed for the cloned $B^0AT1$ or $B^0AT2$, it has been observed in the intact intestine and was already proposed in the kinetic model of Curran et al. (1967; Fig. 1*A*, steps *1-7-5-6*). Model 1C includes two voltage-dependent steps, namely 3 and 6ds. Assigning the charge translocation to the fully loaded transporter explains the absence of trans-stimulation. An exchange process would involve a return trip involving steps *1-2-3-4-5* (or *1a-2a-3-4a-5a*). Acceleration does not occur because return of the fully loaded transporter is slowed down by the membrane potential in step 3. In summary, we propose a multistep model for the mechanism of $B^0AT1$ that is in agreement with the following experimental observations: (i) Substrate binds preferentially first to the transporter; (ii) No trans-stimulation is observed; (iii) A substrate-induced leak current is observed when NaCl is replaced by LiCl. (iv) A substrate-independent $Na^+$-leak current is observed. (v) The transport shows Michaelis-Menten type kinetics for both substrate and cosubstrate. (vi) An inside negative membrane potential increases the $V_{max}$.

## The Neutral Amino Acid Transporter $B^0AT2$ (SLC6A15)

The neutral amino acid transporter $B^0AT2$ has been analyzed in two studies (Takanaga et al., 2005; Broer et al., 2006). The transporter is functionally and sequence related to $B^0AT1$.

### Mechanism

$B^0AT2$ is $Na^+$- but not Cl-dependent; replacement of NaCl by NMDG-Cl completely abolishes transport. Replacement of NaCl by LiCl inhibits transport by 90% in the case of the mouse transporter (Broer et al., 2006) and by about 75% in the human transporter (Takanaga et al., 2005). Substrate-induced currents in LiCl, by contrast, were about 60% of those observed in NaCl. Activation analysis of substrate transport at different $Na^+$ concentrations and flux studies under voltage-clamp indicate a cotransport of 1 $Na^+$ per substrate molecule. Substrate and cosubstrate $K_m$-values are highly voltage dependent, decreasing at hyperpolarized potentials. The $K_m$-value for $Na^+$, for example, decreases from $>50$ mM to 19 mM and to 8.7 mM, when the holding potential is changed from -10 mV to -50 mV and -100 mV, respectively. The $K_m$-value for proline changed from 0.8 mM to 0.2 mM, when the membrane potential changed from $+20$ mV to $-80$ mV (Broer et al., 2006). In addition, the substrate $K_m$ decreases when the $Na^+$ concentration is increased and vice versa.

The mechanistic features of $B^0AT2$ are almost the same as for $B^0AT1$. (i) The substrate $K_m$ decreases with increasing $Na^+$ concentration and vice versa. (ii) Substrate and cosubstrate $K_m$-values decrease at increased hyperpolarization of the membrane. (iii) The maximum velocity increases linearly with hyperpolarization of the membrane. (iv) $Li^+$ causes partial uncoupling of substrate and ion transport. As a result, it appears likely that the kinetic scheme of Fig. 1*C* applies to both $B^0AT1$ and $B^0AT2$.

### Substrate Specificity

$B^0AT2$ mainly transports branched-chain amino acids, methionine and proline with affinities ranging from 40–200 μM. Proline has the highest $V_{max}$ but the $K_m$-values are lower for branched-chain amino acids (Broer et al., 2006). When the catalytic efficiency ($V_{max}/K_m$) is calculated, methionine is the preferred substrate of the transporter (Takanaga et al., 2005). Phenylalanine and alanine are recognized with low

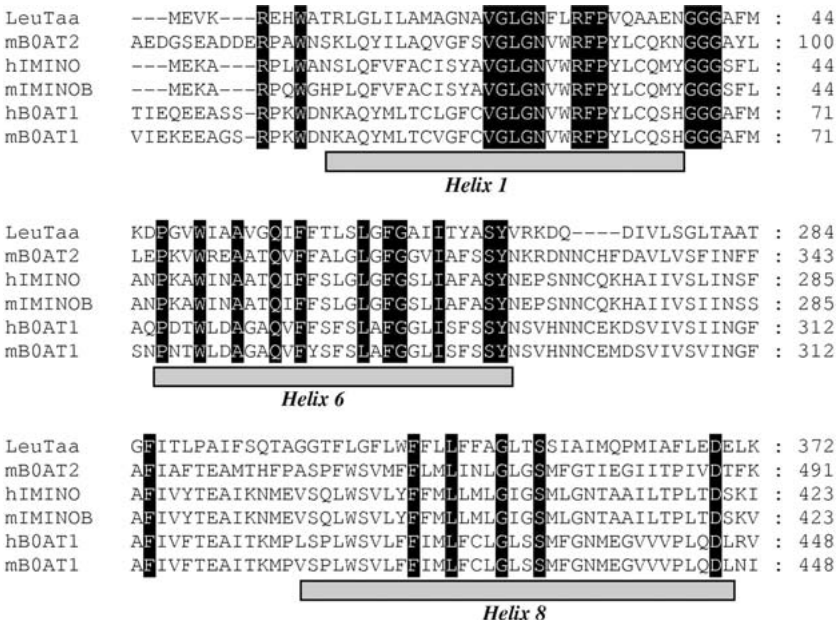


**Fig. 2.** Partial alignment of the primary structure of SLC6 amino acid transporters with the sequence of $LeuT_{Aa}$. Regions including helices 1, 6 and 8 are depicted. Fully conserved residues are shaded in black.

affinity. The transporter is inhibited by high concentrations of BCH, but the compound does not elicit inward currents, suggesting that it is not transported.

## A Proposed Structure of $B^0$-like Amino Acid Transporters

The recently resolved structure of the bacterial amino acid transporter $LeuT_{Aa}$ from *Aquifex aeolicus* provides an unparalleled insight into the structure of transporters from the SLC6 family (Yamashita et al., 2005). The similarity of $LeuT_{Aa}$ to the mammalian neurotransmitter transporters has been emphasized, however, it has to be pointed out that $B^0$-like transporters are functionally closer to $LeuT_{Aa}$ than the neurotransmitter transporters. First, leucine is a substrate of both $LeuT_{Aa}$ and $B^0AT1$ and $B^0AT2$. Secondly, $LeuT_{Aa}$ and both $B^0AT1$ and $B^0AT2$ are $Na^+$-dependent but not $Cl^-$-dependent. The only discrepancy is the presence of two $Na^+$-binding sites in $LeuT_{Aa}$, whereas only one functional binding site is observed in $B^0AT1$ and $B^0AT2$.

Homology modeling, in its simplest form, entails the threading of the primary structure of $B^0AT1$ and $B^0AT2$ along the structure of $LeuT_{Aa}$ (Arnold et al., 2006). However, problems can arise with the insertion or deletion of residues in secondary structure motifs, potentially altering the orientation of the subsequent residues in an α-helix or β-sheet. A more advanced approach used here allows non-aligned residues to be inserted between $LeuT_{Aa}$ backbone residues and the backbone is ligated prior to further threading. The putative structure is energy-minimized and refined, allowing both the backbone atoms and side chains to rotate and adopt a minimum energy conformation, thereby removing unfavorable contacts. As a result, the homology modeling critically relies on a precise alignment of the primary sequence. Fortunately, there is considerable conservation of critical residues throughout the sequence of SLC6 members, particularly in the catalytically important helices 1, 6 and 8 (Fig. 2).

In the following, the key features of the putative $B^0AT2$ structural model are discussed. The $B^0AT2$ model features 12 transmembrane helices, the first ten of which are well aligned with the $LeuT_{Aa}$ sequence. The loops in the bacterial transporter are generally shorter. Because $LeuT_{Aa}$ does not appear to have functional re-entrant loops, the discrepancies in the length of the non-transmembrane loop regions are likely to have little effect on properties such as the substrate specificity or uptake. The lack of homology, nevertheless, creates problems in modeling these extended loop regions. In this case, the extended loop of $B^0AT1$ and $B^0AT2$ between helix 7 and 8 in particular cannot be modeled, as there is no structural information in the $LeuT_{Aa}$ crystal structure for this region. Because of several highly conserved residues in helix 8 (Fig. 2) it is, however, relatively easy to re-align the sequence after the loop, using a combination of primary sequence alignments and secondary structure prediction tools. The modeling process only includes the peptide sequence. Substrate and $Na^+$ ions are reinserted into the structure at the original coordinates. This can cause some malalignment in the area where binding of substrate and cosubstrate occurs. The $B^0AT2$ model, accordingly, contains two $Na^+$-binding sites (Fig. 3 and Fig. 4), whereas functional evidence supports only one binding site (*see* above).

The substrate translocation pathway is lined by helices 1 and 6 (Yamashita et al., 2005). Both helices

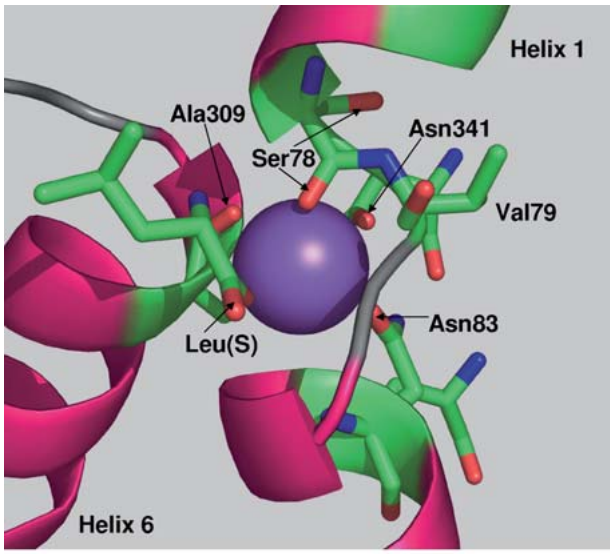


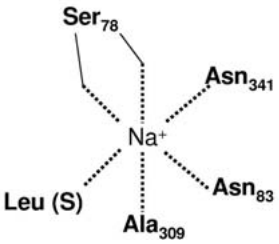


**Fig. 3.** Putative structure of the $Na^+$-binding site 1 in $B^0AT2$. Residues involved in $Na^+$-binding are indicated. A schematic representation of the binding site is given below. The substrate leucine residue is indicated by (*S*). Valine 79 is involved in $Na^+$-binding site 2. Nitrogen atoms have blue color, oxygen atoms are red. The figure was generated using Pymol (DeLano Scientific LLC).

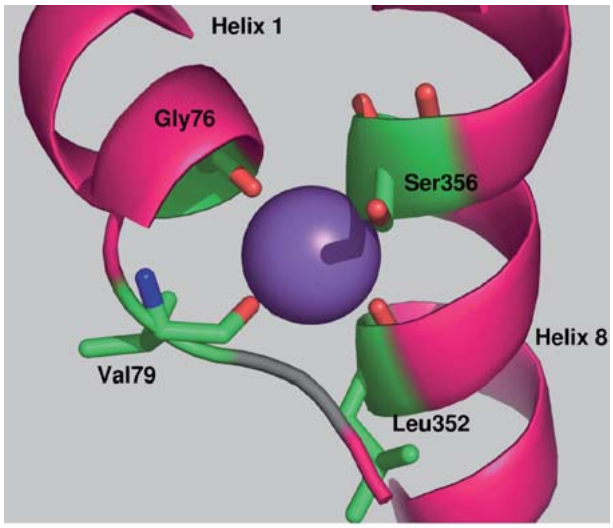


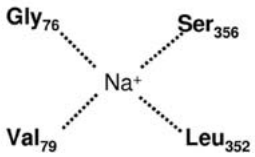


**Fig. 4.** Putative structure of the $Na^+$-binding site 2 in $B^0AT2$. Residues involved in $Na^+$-binding are indicated. A schematic representation of the binding site is given below. Nitrogen atoms have blue color, oxygen atoms are red. The figure was generated using Pymol (DeLano Scientific LLC).

are interrupted by non-α-helical structures in the center of the membrane (Figs. 3 and 4); these form the two $Na^+$ binding sites and the substrate binding site. The flexibility to form these structures is provided by glycine residues. The two $Na^+$ binding sites are qualitatively different. The $Na^+_1$ site (Fig. 3) appears to be well conserved in $B^0AT2$. In the $LeuT_{Aa}$ structure, Thr 254 of helix 6 provides two bonds for $Na^+$ binding, a backbone carbonyl-oxygen and the oxygen of its hydroxyl-group. The corresponding residue in the $B^0AT2$ structure is an alanine, which can only provide the backbone carbonyl-oxygen. This is compensated for by serine 78 in helix 1, which is likely to provide two bonds, whereas $LeuT_{Aa}$ has an alanine residue at position 22 in helix 1 contributing to $Na^+$ binding. It appears likely that the side chain of serine 78 in the $B^0AT2$ model (Fig. 3) points towards $Na^+_1$. Similarly, alanine 309 appears to be slightly out of place. The carboxyl group of the substrate leucine forms part of the $Na^+_1$ binding site. This elegantly explains the mutual effect of substrate and cosubstrate on each other's binding. The $Na^+_2$-binding site is less well conserved (Fig. 4). In the $LeuT_{Aa}$ structure, $Na^+_2$ is fivefold coordinated, whereas only four residues can readily be identified in the putative $B^0AT2$ structure. The hydroxyl-group of serine 474 is likely to point toward the $Na^+$ ion. Similar to ion binding in channels (Gouaux & Mackinnon 2005), negatively charged residues are not involved in $Na^+$-binding, with the exception of the carboxyl group of the substrate leucine. $Na^+$-binding rather relies on electropositive centers, such as carbonyl groups or carboxylamides. Taken together, it is tempting to suggest that $Na^+_1$ is the functional binding site in the $B^0AT2$ structure. It is better conserved and provides an explanation for interdependence of substrate and cosubstrate binding; whether the $Na^+_2$ still exists as a structural center in $B^0AT2$ remains to be demonstrated.

Molecular dynamics simulations indicate that in the $LeuT_{Aa}$ structure substrate and cosubstrate are tightly embedded in the protein core and show little movement (Fig. 5). Indeed, no water molecules contact the buried leucine or sodium ions over 10 ns of molecular dynamics simulation time. This is in agreement with the proposal put forward by Yamashita and co-workers (Yamashita et al. 2005) that substrate and cosubstrate are in an occluded state in the $LeuT_{Aa}$ structure. A chloride ion that is attached peripherally to the structure does not appear

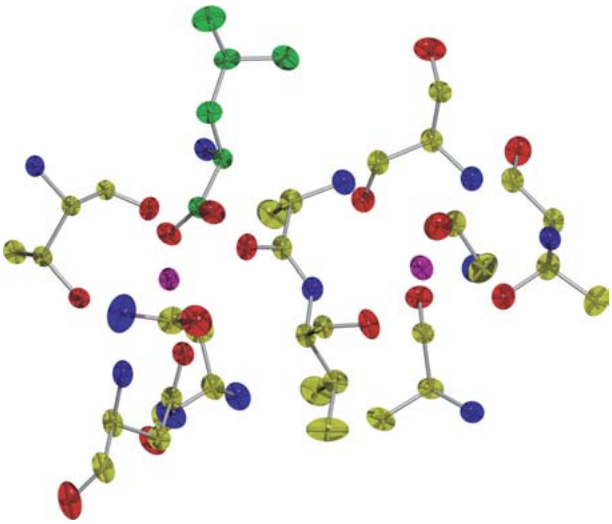

**Fig. 5.** Dynamics of the ligand binding site of $LeuT_{Aa}$. All atoms are represented as spheroids calculated from a 10 ns molecular dynamics simulation. Carbon atoms of $LeuT_{Aa}$ residues are yellow, and those of the leucine substrate are green. Sodium ions are magenta.

to have a critical role, because it immediately diffuses away from its binding site at commencement of the simulation.

The proposed $B^0AT2$ model has a hydrophobic binding pocket (Fig. 6). The substrate leucine side-chain is surrounded by several aromatic amino acids, namely, phenylalanine 77, tryptophan 164, phenylalanine 308 and phenylalanine 314. Other residues contributing to the substrate binding site are valine 160 and threonine 478. Serine 474 is also close to the substrate binding site, but is rather involved in the coordination of $Na_2$ (Fig. 4). In the model, the hydrophilic hydroxyl-group of threonine 478 points away from the binding pocket, whereas the methyl-group points towards the leucine side-chain. The amino group of the substrate leucine could be stabilized by carbonyl groups of phenylalanine 308 and alanine 309 backbones. Please note that the latter residue is also involved in the binding of $Na^+_1$. The amino acid analogue BCH is too large to fit into the proposed substrate binding site. As a result, it can block the entry of other substrates to the transporter, but is not transported itself.

Homology modeling of the $B^0AT2$ structure provides a useful template for future structure-function analysis. The putative $Na^+$ binding site 1 is in good agreement with functional data and so, too, is the hydrophobic binding pocket. The precise spacing is certainly speculative at this stage, but the overall structures of $B^0AT1$ and $B^0AT2$ are likely to be similar to that of $LeuT_{Aa}$.

Work in the laboratory of the authors is supported by grants from the Australian Research Council (ARC) and the National Health and Medical Research Council (NHMRC).

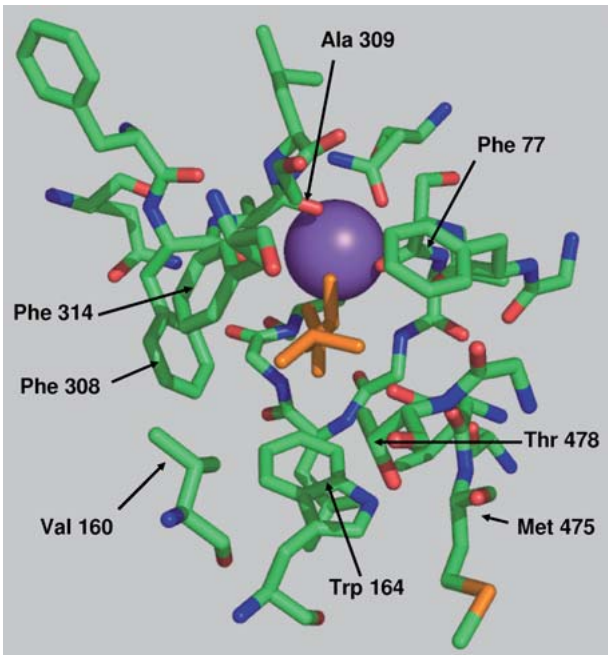


**Fig. 6.** Putative structure of the binding pocket enclosing the side-chain of the $B^0AT2$ substrate leucine, which is shown in orange. In the protein, nitrogen atoms have blue color, oxygen atoms are red. The figure was generated using Pymol (DeLano Scientific LLC).

## References

Arnold, K., Bordoli, L., Kopp, J., Schwede, T. 2006. The SWISS-MODEL workspace: a web-based environment for protein structure homology modelling. *Bioinformatics* **22:**195–201

Binder, H.J. 1970. A comparison of intestinal and renal transport systems. *Am. J. Clin. Nutr.* **23:**330–335

Bohmer, C., Broer, A., Munzinger, M., Kowalczuk, S., Rasko, J.E., Lang, F., Broer, S. 2005. Characterization of mouse amino acid transporter B0AT1 (slc6a19). *Biochem. J.* **389:**745–751

Broer, A., Klingel, K., Kowalczuk, S., Rasko, J.E., Cavanaugh, J., Broer, S. 2004. Molecular cloning of mouse amino acid transport system B0, a neutral amino acid transporter related to Hartnup disorder. *J. Biol. Chem.* **279:**24467–24476

Broer, A., Tietze, N., Kowalczuk, S., Chubb, S., Munzinger, M., Bak, L.K., Broer, S. 2006. The orphan transporter v7–3 (slc6a15) is a $Na^+$-dependent neutral amino acid transporter (B0AT2). *Biochem. J.* **393:**421–430

Camargo, S.M., Makrides, V., Virkki, L.V., Forster, I.C., Verrey, F. 2005. Steady-state kinetic characterization of the mouse B(0)AT1 sodium-dependent neutral amino acid transporter. *Pfluegers Arch.* **451:**338–348

Cohen, L.L., Huang, K.C. 1964. Intestinal Transport Of Tryptophan And Its Derivatives. *Am. J. Physiol.* **206:**647–652

Crane, R.K. 1965. Na+ -dependent transport in the intestine and other animal tissues. *Fed Proc* **24:**1000–1006

Curran, P.F., Schultz, S.G., Chez, R.A., Fuisz, R.E. 1967. Kinetic relations of the Na-amino acid interaction at the mucosal border of intestine. *J. Gen. Physiol.* **50:**1261–1286

Cusworth, D.C., Dent, C.E. 1960. Renal clearances of amino acids in normal adults and in patients with aminoaciduria. *Biochem J.* **74:**550–561

Doyle, F.A., McGivan, J.D. 1992. The bovine renal epithelial cell line NBL-1 expresses a broad specificity Na(+)-dependent neutral amino acid transport system (System Bo) similar to that

in bovine renal brush border membrane vesicles. *Biochim. Biophys. Acta.* **1104:**55–62

Evers, J., Murer, H., Kinne, R. 1976. Phenylalanine uptake in isolated renal brush border vesicles. *Biochim. Biophys. Acta.* **426:**598–615

Fass, S.J., Hammerman, M.R., Sacktor, B. 1977. Transport of amino acids in renal brush border membrane vesicles. Uptake of the neutral amino acid L-alanine. *J. Biol. Chem.* **252:**583–590

Fox, M., Thier, S., Rosenberg, L., Segal, S. 1964. Ionic requirements for amino acid transport in the rat kidney cortex slice. I. Influence of extracellular ions. *Biochim. Biophys. Acta.* **79:**167–176

Gouaux, E., Mackinnon, R. 2005. Principles of selective ion transport in channels and pumps. *Science* **310:**1461–1465

Hoyer, J., Gogelein, H. 1991. Sodium-alanine cotransport in renal proximal tubule cells investigated by whole-cell current recording. *J. Gen. Physiol.* **97:**1073–1094

Kleta, R., Romeo, E., Ristic, Z., Ohura, T., Stuart, C., Arcos-Burgos, M., Dave, M.H., Wagner, C.A., Camargo, S.R., Inoue, S., et al. 2004. Mutations in SLC6A19, encoding B0AT1, cause Hartnup disorder. *Nat. Genet.* **36:**999–1002

Kragh-Hansen, U., Roigaard-Petersen, H., Jacobsen, C., Sheikh, M.I. 1984. Renal transport of neutral amino acids. Tubular localization of $Na^+$-dependent phenylalanine- and glucose-transport systems. *Biochem. J.* **220:**15–24

Mircheff, A.K., Kippen, I., Hirayama, B., Wright, E.M. 1982. Delineation of sodium-stimulated amino acid transport pathways in rabbit kidney brush border vesicles. *J. Membrane. Biol.* **64:**113–122

Murer, H., Sigrist-Nelson, K., Hopfer, U. 1975. On the mechanism of sugar and amino acid interaction in intestinal transport. *J. Biol. Chem.* **250:**7392–7396

Nelson, N., Sacher, A., Nelson, H. 2002. The significance of molecular slips in transport systems. *Nature Rev. Mol. Cell. Biol.* **3:**876–881

Palacin, M., Nunes, V., Font-Llitjos, M., Jimenez-Vidal, M., Fort, J., Gasol, E., Pineda, M., Feliubadalo, L., Chillaron, J., Zorzano, A. 2005. The genetics of heteromeric amino acid transporters. *Physiology (Bethesda)* **20:**112–124

Paterson, J.Y., Sepulveda, F.V., Smith, M.W. 1979. Two-carrier influx of neutral amino acids into rabbit ileal mucosa. *J. Physiol.* **292:**339–350

Paterson, J.Y., Sepulveda, F.V., Smith, M.W. 1981. Distinguishing transport systems having overlapping specificities for neutral and basic amino acids in the rabbit ileum. *J. Physiol.* **319:**345–354

Potter, S.J., Lu, A., Wilcken, B., Green, K., Rasko, J.E. 2002. Hartnup disorder: polymorphisms identified in the neutral amino acid transporter SLC1A5. *J. Inherit. Metab. Dis.* **25:**437–448

Preston, R.L., Schaeffer, J.F., Curran, P.F. 1974. Structure-affinity relationships of substrates for the neutral amino acid transport system in rabbit ileum. *J. Gen. Physiol.* **64:**443–467

Reiser, S., Christiansen, P.A. 1967. Intestinal transport of valine as affected by ionic environment. *Am. J. Physiol.* **212:**1297–1302

Samarzija, I., Fromter, E. 1982. Electrophysiological analysis of rat renal sugar and amino acid transport. III. Neutral amino acids. *Pfluegers Arch.* **393:**119–209

Schultz, S.G., Alvarez, O.O., Curran, P.F., Yu-Tu, L. 1970. Dicarboxylic amino acid influx across brush border of rabbit ileum. Effects of amino acid charge on the sodium-amino acid interaction. *J. Gen. Physiol.* **56:**621–639

Schultz, S.G, Curran, P.F. 1970. Coupled transport of sodium and organic solutes. *Physiol. Rev.* **50:**637–718

Schultz, S.G., Curran, P.F., Chez, R.A., Fuisz, R.E. 1967. Alanine and sodium fluxes across mucosal border of rabbit ileum. *J. Gen. Physiol.* **50:**1241–1260

Scriver, C.R., Mohyuddin, F. 1968. Amino acid transport in kidney. Heterogeneity of alpha-aminoisobutyric uptake. *J. Biol. Chem.* **243:**3207–3213

Segal, S., Crawhall, J.C. 1968. Characteristics of cystine and cysteine transport in rat kidney cortex slices. *Proc. Natl. Acad. Sci. USA* **59:**231–237

Seow, H.F., Broer, S., Broer, A., Bailey, C.G., Potter, S.J., Cavanaugh, J.A., Rasko, J.E. 2004. Hartnup disorder is caused by mutations in the gene encoding the neutral amino acid transporter SLC6A19. *Nat. Genet.* **36:**1003–1007

Stein, W.D. 1986. Transport and Diffusion Across Cell Membranes. Academic Press, San Diego

Takanaga, H., Mackenzie, B., Peng, J.B., Hediger, M.A. 2005. Characterization of a branched-chain amino-acid transporter SBAT1 (SLC6A15) that is expressed in human brain. *Biochem. Biophys. Res. Commun.* **337:**892–900

Ullrich, K.J., Rumrich, G., Kloss, S. 1974. Sodium dependence of the amino acid transport in the proximal convolution of the rat kidney. *Pfluegers Arch.* **351:**49–60

Yamashita, A., Singh, S.K., Kawate, T., Jin, Y., Gouaux, E. 2005. Crystal structure of a bacterial homologue of Na(+)/Cl(−)-dependent neurotransmitter transporters. *Nature* **437:**215–223